

This document is the Accepted Manuscript version of a Published Work that appeared in final form in Macromolecules, copyright © American Chemical Society after peer review and technical editing by publisher. To access the final edited and published work see <https://dx.doi.org/10.1021/acs.macromol.7b00527>

Long-Range, Polymer Chain Dynamics of a ‘Stiff’ Polymer. Fluorescence from Poly(isobutylene-*alt*-maleic anhydride) with *N*-(1-Pyrenylmethyl)succinimide Groups

Janine L. Thoma, Jean Duhamel*

Institute for Polymer Research, Waterloo Institute for Nanotechnology, Department of Chemistry, University of Waterloo, Waterloo, ON N2L 3G1, Canada

Mei-Jin Li,^{a,b} Michael J. Bertocchi,^b Richard G. Weiss^{b,c,*}

^a Key Laboratory of Analysis and Detection Technology for Food Safety (Ministry of Education and Fujian Province), Department of Chemistry, Fuzhou University, Fuzhou 350116, P. R. China

^b Department of Chemistry and ^c Institute for Soft Matter Synthesis and Metrology, Georgetown University, Washington, D.C. 20057-1227, USA

ABSTRACT

The steady-state fluorescence (SSF) spectra and time-resolved fluorescence (TRF) decays of five poly(isobutylene-*alt*-maleic anhydride) copolymers (PIMA), randomly labeled with *N*-(1-pyrenylmethyl)succinimide groups (Py-PIMA), have been analyzed in order to describe their long-range, polymer chain dynamics (LRPCD) and to assess the stiffness of the PIMA backbone compared to that of a series of poly(alkyl methacrylate)s whose LRPCD had already been investigated. The SSF spectra, recorded under dilute concentration conditions where only *intrachain* events are important, show that the intensity ratio of pyrenyl excimer to pyrenyl monomer emission (i.e., $(I_E/I_M)^{SSF}$) increases linearly with increasing pyrenyl content as a result of increased pyrenyl-pyrenyl contacts and diffusive encounters. The slope of the straight line, $m(I_E/I_M)$, that reflected the efficiency of pyrenyl excimer formation for Py-PIMA, was found to be 60% smaller than for even poly(octadecyl methacrylate) (PC18MA), a polymer exhibiting slow LRPCD due to its long, bulky side chain. Analyses of the SSF spectra allowed separation of the averaged behaviour of five different pyrenyl species in the Py-PIMA polymers, although only two of them were reflected in the LRPCD of PIMA. In addition, the fluorescence decays of the pyrenyl monomer and excimer, when fitted globally according to the model free analysis (MFA), yielded the average rate constant $\langle k^{MF} \rangle^{blob}$ of pyrenyl excimer formation that directly represents the LRPCD of Py-PIMA. After having conducted two tests that confirmed the validity of the parameters retrieved from the MFA of the TRF decays, $\langle k^{MF} \rangle^{blob}$ for Py-PIMA was compared to $\langle k^{MF} \rangle^{blob}$ of 9 other polymers. The result of this comparison leads us to conclude that the PIMA backbone is extremely stiff in THF. This study demonstrates the ability of the MFA of fluorescence decays acquired from polymers randomly labeled with pyrenyl groups to characterize quantitatively the LRPCD of even extremely stiff polymers.

INTRODUCTION

The traditional procedure to probe long range, polymer chain dynamics (LRPCD) in solution by fluorescence is to select two chromophores with the ability to communicate spectroscopically with one another and covalently attach them to the ends of a monodisperse polymer. Labels such as chromophore pairs capable of undergoing Fluorescence Resonance Energy Transfer (FRET)¹⁻⁴ and pyrenyl groups that can readily undergo excimer formation^{5,6} have been often selected for this purpose. In these experiments, the rate constant k_q , reflecting the photophysical process by which the excited chromophore at one end of the chain is being quenched dynamically by the ground-state chromophore at the other end of the chain, is measured through the analysis of time-resolved fluorescence (TRF) decays.¹⁻⁶ The rate constant k_q is then related to the end-to-end cyclization (EEC) rate constant k_{cy} of the polymer of interest, which is then recorded as a function of the degree of polymerization of a polymer (DP). The k_{cy} -versus-DP trends obtained for different polymers enable, in theory, one to compare the k_{cy} values and to use them to rank the relative stiffness of different polymer backbones.^{6,7}

Although this procedure has been used for decades to gain information about the LRPCD of end-labeled oligomers with a few tens of structural units, a recent review has pointed out that it is poorly suited to study real polymers with DP values greater than 100.⁶ This conclusion follows from the steep decrease in k_{cy} with increasing DP, which leads to a minuscule number of EEC events when DP is much larger than 100. In effect, polymers with a backbone stiffer than polystyrene are expected to be too rigid to study by monitoring their EEC by fluorescence. Furthermore, the construction of the k_{cy} -versus-DP trends is very demanding synthetically so that such plots are rarely generated in practice. Finally, the study of EEC is obviously impossible to

conduct with polymers whose end groups cannot be readily reacted with a fluorescent derivative. These considerations have been discussed in several reviews.^{6,8,9}

Consequently, the LRPCD of alternating copolymers of isobutylene and maleic anhydride (PIMA), obtained by free radical polymerization, would be impossible to determine by EEC experiments. PIMA does not exhibit end groups that can be readily reacted with fluorescent derivatives and the anhydride groups are rigid structural units that are expected to slow the LRPCD to the point where too few EEC events would be observed. Although end-labeling of PIMA does not seem to be a viable option, its anhydride units could be easily reacted with 1-pyrenylmethylamine to generate *N*-(1-pyrenylmethyl)succinimide moieties randomly distributed along the PIMA chain, thus yielding Py-PIMA polymers (Table 1) in which a nitrogen atom is present in the linker at the position β to pyrenyl and that the pyrenyl label is three atoms from the main chain. These molecular parameters have been found to be most important for the characterization of the LRPCD of pyrenyl-labeled macromolecules (PyLMs).^{10,11} In turn, the LRPCD of polymers randomly labeled with pyrenyl groups can be characterized by applying the global Model Free Analysis (MFA) to the monomer and excimer TRF decays.¹²⁻¹⁵

The repeat structure of PIMA suggests a very rigid polymer backbone. To demonstrate that the LRPCD of such a polymer can be characterized by randomly labeling its backbone with pyrenyl derivatives and characterize their fluorescence decays, the MFA was applied to a series of Py-PIMA constructs with different degrees of *N*-(1-pyrenylmethyl)succinimide substitution to quantify the LRPCD of the PIMA backbone in THF. The Py-PIMA polymers were found to behave similarly to many other polymers randomly labeled with pyrenyl groups, but with the special feature that they formed very little excimer at the same pyrenyl content as those appended to the more flexible backbones of polystyrene,^{16,17} poly(alkyl methacrylate)s,¹⁸ or polyacrylamides.^{19,20}

This observation, together with the small average rate constant $\langle k \rangle$ of pyrenyl excimer formation retrieved from the MFA of the Py-PIMA decays, leads us to conclude that the PIMA backbone is, in fact, significantly stiffer than any other polymer with a low molecular weight structural unit that has been studied to date. These results support the claim made earlier^{8,9} that MFA of the TRF decays acquired with polymers randomly labeled with pyrenyl can yield quantitative information about the LRPCD of any pyrenyl-labeled macromolecule (PyLM), including those with linear chain and stiff backbones.

EXPERIMENTAL

Materials: Distilled in glass tetrahydrofuran (THF) was purchased from Caledon. The synthesis of the Py-PIMA samples with pyrenyl content of 0.5, 5, 10, 25, and 47.5 mol% with respect to the number of structural units was achieved by reacting 1-pyrenemethyl amine with PIMA (Aldrich, $M_w \sim 6,000 \text{ g}\cdot\text{mol}^{-1}$) and has been reported earlier.²¹

UV-Vis absorption: The UV-Vis absorption spectra of the Py-PIMA solutions in THF were recorded with a Varian Cary 100 Bio spectrophotometer to ensure that the polymer solutions in THF were prepared with a same $\sim 2.5 \times 10^{-6} \text{ M}$ concentration in pyrenyl labels. This low polymer concentration prevented the occurrence of *interchain* excimer formation, as demonstrated by the constancy of the I_E/I_M ratio for solutions of one polymer type at pyrenyl concentrations as high as $1 \times 10^{-5} \text{ M}$.²¹

Steady-state fluorescence measurements: The SSF spectra were acquired at a right angle geometry on a Photon Technology International LS-100 steady-state fluorometer with an Ushio UXL-75 Xenon lamp and a PTI 814 photomultiplier detection system. The excitation wavelength was set at 344 nm and the spectra were recorded from 350 to 600 nm using a scanning rate of 10 nm/min.

The Py-PIMA solutions in THF were deoxygenated for 30 min under a gentle flow of nitrogen. The SSF spectra were analyzed by integrating the fluorescence intensity between 372 and 378 nm for the pyrenyl monomer and between 500 and 530 nm for the pyrenyl excimer to yield the fluorescence intensity I_M and I_E , respectively. These intensities were used to calculate the fluorescence intensity ratios $(I_E/I_M)^{SSF}$.

Time-resolved fluorescence measurements: The TRF decays were acquired on an IBH Ltd. time-resolved fluorometer fitted with an IBH 340 nm NanoLED to excite the Py-PIMA solutions in THF. The N₂-saturated solutions used to acquire the SSF spectra were then employed to acquire the TRF decays of the pyrenyl monomer and excimer by exciting the solutions at 344 nm and monitoring the fluorescence intensity versus time at either 375 nm for the monomer or 510 nm for the excimer. To reduce scattered light from reaching the detector, a 370 or 495 nm cut-off filter was placed in front of the emission monochromator to obtain the monomer and excimer fluorescence decays, respectively. The fluorescence decays had a minimum of 20,000 counts at the decay maximum and were acquired over 1,024 channels with a 1.02 or 2.04 nanosecond-per-channel, depending on the pyrenyl content of the Py-PIMA samples. Analyses of the monomer and excimer decays were conducted globally with the MFA, and the fits were deemed satisfactory if the χ^2 parameter was smaller than 1.20 and the residuals and autocorrelation of the residuals were randomly distributed around zero.

Global Model Free Analysis of the monomer and excimer fluorescence decays: The TRF decays of the pyrenyl monomer and excimer were fitted globally according to the MFA. As usually done when excimer formation occurs between pyrenyl labels that are sterically constrained, and as is the case for the Py-PIMA samples, the MFA treatment assumed the existence of five pyrenyl species in solution: those isolated along the PIMA chain that do not form excimer (Py_{free}^*); those

that diffusively encounter a ground-state pyrenyl monomer to form a properly stacked excimer ($E0^*$) or an improperly stacked excited dimer (D^*) and referred to as Py_{diffE0}^* and Py_{diffD}^* , respectively; and those that are aggregated and lead to the quasi-instantaneous formation of an excimer $E0^*$ or an excited dimer D^* upon direct excitation. The pyrenyl species Py_{free}^* , Py_{diffE0}^* , and Py_{diffD}^* contributed to the monomer decays whereas the pyrenyl species Py_{diffE0}^* , Py_{diffD}^* , $E0^*$, and D^* contributed to the excimer decays. The monomeric species, Py_{free}^* , Py_{diffE0}^* , and Py_{diffD}^* had a lifetime, τ_M , and the excimer $E0^*$ and long-lived excited dimer D^* had lifetimes of τ_{E0} and τ_D , respectively. Equations 1 and 2 were used to fit the monomer and excimer decays.

$$[Py^*]_{(t)} = ([Py_{diffE0}^*]_{(t=0)} + [Py_{diffD}^*]_{(t=0)}) \times \sum_{i=1}^n a_i \times \exp(-t/\tau_i) + [Py_{free}^*]_{(t=0)} \times \exp(-t/\tau_M) \quad (1)$$

$$\begin{aligned}
[E^*]_{(t)} = & -[Py_{diffE0}^*]_{(t=0)} \times \sum_{i=1}^n a_i \frac{\frac{1}{\tau_i} - \frac{1}{\tau_{E0}}}{\frac{1}{\tau_i} - \frac{1}{\tau_M}} \exp(-t/\tau_i) \\
& + \left([E0^*]_{(t=0)} + [Py_{diffE0}^*]_{(t=0)} \times \sum_{i=1}^n a_i \frac{\frac{1}{\tau_i} - \frac{1}{\tau_{E0}}}{\frac{1}{\tau_i} - \frac{1}{\tau_M}} \right) \times \exp(-t/\tau_{E0}) \\
& - [Py_{diffD}^*]_{(t=0)} \times \sum_{i=1}^n a_i \frac{\frac{1}{\tau_i} - \frac{1}{\tau_D}}{\frac{1}{\tau_i} - \frac{1}{\tau_M}} \exp(-t/\tau_i) \\
& + \left([D^*]_{(t=0)} + [Py_{diffD}^*]_{(t=0)} \times \sum_{i=1}^n a_i \frac{\frac{1}{\tau_i} - \frac{1}{\tau_D}}{\frac{1}{\tau_i} - \frac{1}{\tau_M}} \right) \times \exp(-t/\tau_D) \quad (2)
\end{aligned}$$

Equation 1 assumed that the monomers $P_{y_{\text{diff}E0^*}}$ and $P_{y_{\text{diff}D^*}}$ formed the excimer $E0^*$ and excited dimer D^* in the same manner and could thus be described by a same sum of exponentials whose pre-exponential factors were normalized to unity ($\sum_{i=1}^n a_i = 1$). In Equation 2, the excimer and the excited dimer have lifetimes τ_{E0} and τ_D , respectively. The monomer and excimer decays were fitted globally according to Equations 1 and 2 and the parameters were optimized with the Marquardt-Levenberg algorithm. The mathematical procedure employed to calculate the molar fractions, f_{free} , $f_{\text{diff}E0}$, $f_{\text{diff}D}$, f_{E0} , and f_D for, respectively, the pyrenyl species, $P_{y_{\text{free}^*}}$, $P_{y_{\text{diff}E0^*}}$, $P_{y_{\text{diff}D^*}}$, $E0^*$, and D^* is provided as Supporting Information. More information about the MFA can be obtained in the original publications¹²⁻¹⁵ and more recent reviews.^{6,8,9}

RESULTS AND DISCUSSION

The SSF spectra of the Py-PIMA samples, acquired under dilute conditions in THF (Figure 1A), exhibited the features expected from a pyrenyl-labeled polymer that forms excimers. The sharp fluorescence peaks between 370 and 410 nm are characteristic of the pyrenyl monomer, while the broad, structureless emission centered at 475 nm is indicative of the excimer. As the molar fraction (x) of structural units bearing a pyrenyl label in the Py-PIMA sample was increased from 0.005 to 0.475, more excimer was produced, as reflected by the increased excimer emission at 475 nm (Figure 1A).

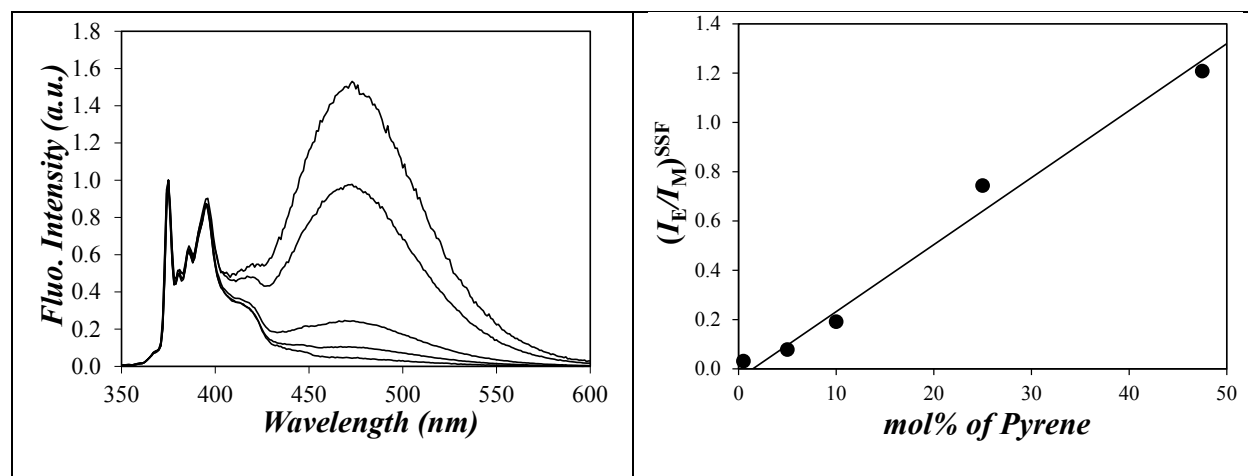


Figure 1. A) Fluorescence spectra of the Py-PIMA sample in THF normalized at the 0-0 transition at 375 nm. From bottom to top: $x = 0.005, 0.05, 0.10, 0.25,$ and 0.475 . $\lambda_{\text{ex}} = 344$ nm. B) Plot of $(I_E/I_M)^{\text{SSF}}$ as a function of the molar percentage of pyrenyl labeled structural units in the Py-PIMA samples.

The fluorescence intensities of the monomer and excimer emissions were used to determine the $(I_E/I_M)^{\text{SSF}}$ ratios. A plot of $(I_E/I_M)^{\text{SSF}}$ versus the molar fraction of pyrenyl groups x in the copolymer yielded a straight line (Figure 1B). Its slope, $m(I_E/I_M)$ equal to 0.027 ± 0.003 , is a measure of the efficiency of pyrenyl excimer formation for the Py-PIMA samples. However, the intercept of the straight line for the plot in Figure 1B does not pass through zero, as is usually the case for polymers randomly labeled with pyrenyl groups.¹⁸ This observation is a result of the requirement that a minimum number of pyrenyl labels must be present in the polymer to be able to form an excimer. Above this minimum pyrenyl content, excimer formation increases with increasing pyrenyl content, as is observed.

Ideally, $m(I_E/I_M)$ could be used to compare the internal dynamics of different polymeric backbones, such that a polymer with a lower $m(I_E/I_M)$ value would have a stiffer backbone than a polymer with a higher $m(I_E/I_M)$ value. In practice, such a comparison is complicated by the need

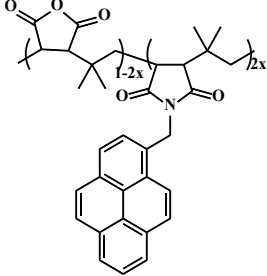
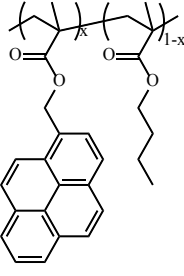
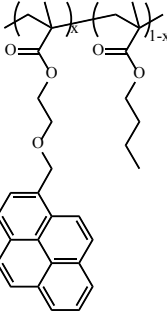
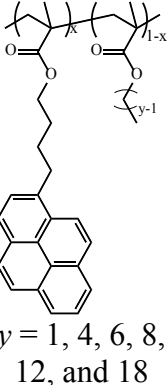
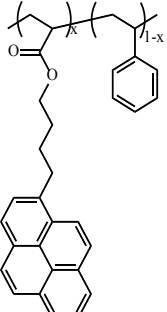
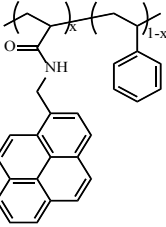
to account for a number of molecular parameters, particularly the length of the spacer linking pyrenyl to the main chain,^{11,16,17} and whether a heteroatom like oxygen or nitrogen is present in the linker at the position β to the pyrenyl label.¹⁰ In the case of poly(butyl methacrylate) labeled by copolymerizing butyl methacrylate with either 1-pyrenylmethyl methacrylate (PyMeO-X(3)-PC4MA, a 3-atom linker) or 1-pyrenylmethoxyethyl methacrylate (PyMeO-X(6)-PC4MA, a 6-atom linker), $m(I_E/I_M)$ doubled from 0.10 to 0.22 upon increasing the linker length from 3 to 6 atoms.¹¹ The chemical structures of the different polymers used in this discussion are provided in Table 1. Increasing the linker length enables the pyrenyl label to probe a larger volume during its excited singlet state lifetime, reduces steric hindrance from the main chain, and, thus, facilitates pyrenyl excimer formation which results in a larger $m(I_E/I_M)$ slope.

Another point to consider when interpreting the magnitude of $(I_E/I_M)^{SSF}$ ratios is that the presence of a heteroatom at the position β to pyrenyl in the linker has been found to restore the ability of the 0-0 transition of pyrene to respond to the polarity of the environment.¹⁰ In practice, its effect is to lower the fluorescence intensity of the pyrenyl monomer taken at 375 nm compared to a linker where the heteroatom is replaced by a methylene unit, thus resulting in an increase in $m(I_E/I_M)$. For instance, $m(I_E/I_M)$ decreased almost by half from 0.22 to 0.09 when butyl methacrylate was copolymerized with 1-pyrenylmethoxyethyl (PyMeO-X(6)-PC4MA) or 1-pyrenylbutyl methacrylate (PyBut-X(6)-PC4MA), respectively.¹⁰ These polymers have the same number of atoms in the linker connecting pyrenyl to the main chain so that the effect of the oxygen atom in the position β to pyrenyl could be investigated selectively. Taking into account the doubling in $m(I_E/I_M)$ between PyMeO-X(6)-PC4MA and PyBut-X(6)-PBMA resulting from the presence of a heteroatom in the linker at the β -position to pyrenyl and the halving in $m(I_E/I_M)$ resulting from the loss in mobility due to the linker length reduction between PyMeO-X(3)-PBMA

and PyMeO-X(6)-PBMA, it can be concluded that $m(I_E/I_M)$ values obtained for a same polymer with a PyMeO-X(3) spacer are comparable to those obtained with a PyBut-X(6) spacer.

With its nitrogen atom in the 3-atom linker at the position β to pyrenyl, Py-PIMA should have an $m(I_E/I_M)$ value that can be compared to that of polymers labeled with PyMeO-X(3) or PyBut-X(6). As mentioned, the $m(I_E/I_M)$ value of 0.027 obtained for Py-PIMA is much smaller than the $m(I_E/I_M)$ values of 0.10 and 0.09 obtained for PyMeO-X(3)-PC4MA and PyBut-X(6)-PC4MA, suggesting that PIMA has a much stiffer backbone than PC4MA. This result is reasonable considering that the cyclic anhydrides are part of the PIMA backbone and seriously constrain its mobility. In fact, the $m(I_E/I_M)$ value of 0.027 for PIMA is even smaller than the 0.043 ± 0.003 and 0.045 ± 0.003 values for PyBut-X(6)-PC12MA (poly(lauryl methacrylate)) and PyBut-X(6)-PC18MA (poly(stearyl methacrylate)).¹⁸ Before the current research, 0.044 was considered to be the lowest value of $m(I_E/I_M)$ possible with poly(alkyl methacrylates) having very long alkyl side chains. Thus, based on the SSF results, the PIMA backbone appears to be about 60% stiffer than the backbone of the most sterically hindered poly(alkyl methacrylate)s exhibiting the slowest internal dynamics of the poly(alkyl methacrylate) series studied in an earlier publication.¹⁸

Table 1. Chemical structures of the pyrenyl-labeled polymers whose photophysical properties are discussed in the analysis of the SSF spectra and TRF decays.

Py-PIMA	PyMeO-X(3)-PC4MA	PyMeO-X(6)-PC4MA	PyBut-X(6)-PCyMA	PyBut-X(6)-PS	PyMeN-X(3)-PS
					

An analysis of long range, polymer chain dynamics (LRPCD) based on $m(I_E/I_M)$ is interesting but it remains limited by a number of complications. We have already alluded to the care that must be taken to the nature of the linker connecting the pyrenyl label to the polymer backbone and the importance of its length and the presence of a heteroatom in a position β to the pyrenyl group. Another problem is that the fluorescence signal emitted by a pyrenyl-labeled macromolecule (PyLM) is the result of no less than five pyrenyl species, as discussed in the Experimental. These are the pyrenyl labels that are isolated along the chain and cannot form an excimer (Py_{free}^*), that diffuse within the polymer coil to encounter a ground-state pyrenyl group, and form a properly stacked excimer (Py_{diffE0}^*) or an improperly stacked long-lived excited dimer (Py_{diffD}^*), and that are pre-stacked and form either an excimer ($E0^*$) or a long-lived excited dimer (D^*) via direct excitation. These different pyrenyl species are defined by their excited singlet state lifetimes (τ_M for the three pyrenyl monomer species Py_{free}^* , Py_{diffE0}^* , and Py_{diffD}^* , τ_{E0} for a properly stacked excimer $E0^*$, and τ_D for the improperly stacked long-lived excited dimers D^*),

their molar fractions (f_{free} , f_{diffE0} , f_{diffD} , f_{E0} , and f_{D}), and the average rate constant $\langle k \rangle$ for pyrenyl excimer formation. Typically, the molar fractions of pyrenyl species that form excimer by diffusion or are aggregated are referred to as $f_{\text{diff}} = f_{\text{diffE0}} + f_{\text{diffD}}$ and $f_{\text{agg}} = f_{\text{E0}} + f_{\text{D}}$, respectively. Based on this discussion, PyLMs with a low pyrenyl content have a large population of isolated pyrenyl groups, P_{yfree}^* , that cannot form excimer and the fluorescence signal of the pyrenyl monomer is dominated by that species. On the other hand, PyLMs with a high pyrenyl content have a large population of aggregated pyrenyl groups (E0^* and D^*) whose fluorescence signal interferes with that of the excimer formed by diffusion. Yet, a study of LRPCD is only concerned with the pyrenyl species that form excimer by diffusion, conditions that would correspond to f_{diff} being equal to unity. Unfortunately, an analysis based on the $(I_{\text{E}}/I_{\text{M}})^{\text{SSF}}$ ratio is unable to distinguish between the different pyrenyl species present in solution and provides only an average representation of LRPCD. These considerations matter particularly in the present case where the stiff PIMA backbone requires that very high pyrenyl contents be used to generate sufficient excimer for the characterization of LRPCD. Under such conditions, f_{agg} is bound to increase with increasing pyrenyl content leading f_{diff} to depart from unity.

While the above discussion introduces some doubt about the validity of an analysis of LRPCD based solely on SSF, work from the Waterloo laboratory has established that these problems are eliminated when the time-resolved fluorescence (TRF) decays of the pyrenyl monomer and excimer of a PyLM are considered instead of its SSF spectra.^{13-15,22} The methodology uses the model free analysis (MFA) to fit the monomer and excimer fluorescence decays globally. Each pyrenyl species is assigned a specific lifetime and molar fraction, and any decrease in monomer fluorescence intensity that cannot be traced back to its natural decay with its lifetime τ_{M} is attributed to excimer formation by diffusion that must be matched by an increase in

excimer fluorescence in the excimer fluorescence decay. In so doing, the MFA retrieves the molar fractions of all pyrenyl species that contribute to the monomer decay (i.e., $f_{M_{\text{free}}}$, $f_{M_{\text{diffE0}}}$, and $f_{M_{\text{diffD}}}$ for Py_{free}^* , Py_{diffE0}^* , and Py_{diffD}^*), to the excimer decay (i.e., $f_{E_{\text{diffE0}}}$, $f_{E_{\text{diffD}}}$, f_{E0} , and f_{ED} for Py_{diffE0}^* , Py_{diffD}^* , $E0^*$, and D^*), the lifetimes τ_{E0} and τ_D , and the decay times τ_i and pre-exponential factors a_i used in Equation 1 to describe pyrenyl excimer formation by diffusion. The molar fractions can then be rearranged to yield the overall molar fractions (f_{free} , f_{diffE0} , f_{diffD} , f_{E0} , and f_D) as shown in Supporting Information. All parameters retrieved from the MFA of the fluorescence decays have been listed in Tables S1-3 of the Supporting Information. The fluorescence decays of the pyrenyl monomer and excimer of dilute solutions of the four Py-PIMA samples with perceptible excimer emission in THF were acquired and fitted according to the MFA. The monomer lifetime τ_M was obtained by fitting the TRF decays of the pyrenyl monomer of the 0.005 molar fraction substituted Py-PIMA with two exponentials. The long-lived exponential was retrieved with a 87% contribution and a decay time of 270 ns that was attributed to τ_M . Using $\tau_M = 270$ ns, the global fits of the monomer and excimer decays with Equations 1 and 2 were excellent, as illustrated in Figure 2 and the results from these fits are now discussed.

Among the numerous advantages offered by the MFA is that its results must conform to a number of verifications in order to confirm the validity of the retrieved parameters. First, the parameters listed in Tables S1-3 can be rearranged using Equation 3 to yield the absolute $(I_E/I_M)^{\text{TRF}}$ ratios. The equations used to determine $\langle \tau \rangle$, the average decay time of Py_{diff}^* , and $\langle k \rangle$ in Equation 3 are given in Equations 4 and 5, respectively. The parameters a_i and τ_i used to determine $\langle \tau \rangle$ in Equation 4 are the normalized pre-exponential factors and decay times used to fit the monomer decays with Equation 1.

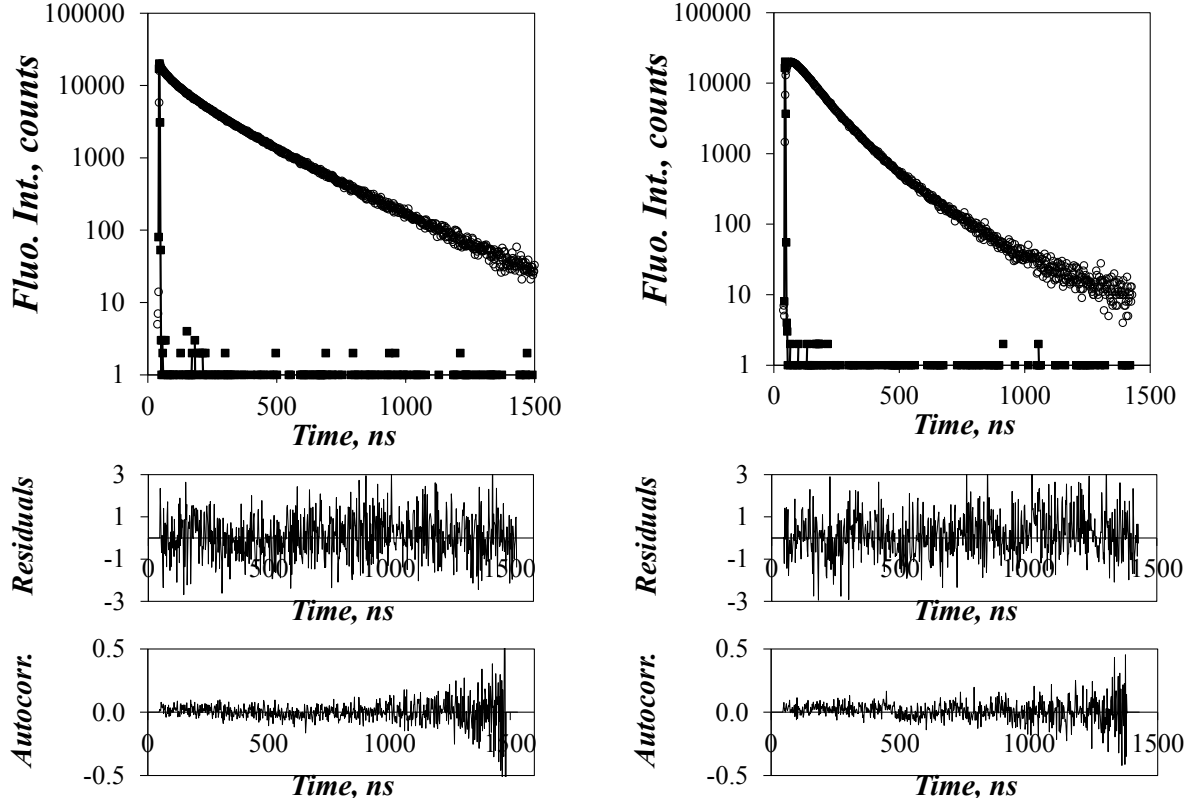


Figure 2. Result of the global MFA of the pyrenyl monomer (left, $\lambda_{em} = 375$ nm) and excimer (right, $\lambda_{em} = 510$ nm) fluorescence decays of Py-PIMA with 0.05 molar fraction of pyrenyl substitution in THF. $\lambda_{ex} = 344$ nm; $\chi^2 = 1.01$.

$$(I_E/I_M)^{TRF} = \frac{(f_{diffE0} \times \tau_{E0} + f_{diffD} \times \tau_D) \times \langle \tau \rangle + f_{E0} \times \tau_{E0} + f_D \times \tau_D}{f_{diff} \langle \tau \rangle + f_{free} \tau_M} \quad (3)$$

$$\langle \tau \rangle = \sum_{i=1}^3 a_i \tau_i \quad (4)$$

$$\langle k \rangle = \frac{1}{\langle \tau \rangle} - \frac{1}{\tau_M} \quad (5)$$

In turn, the absolute $(I_E/I_M)^{\text{TRF}}$ ratios are expected to be proportional to the relative $(I_E/I_M)^{\text{SSF}}$ ratio already reported in Figure 1B. That this is indeed the case is illustrated in Figure 3A where $(I_E/I_M)^{\text{TRF}}$ is shown to increase linearly with $(I_E/I_M)^{\text{SSF}}$. The second check that must be applied to validate the results obtained from the MFA is to verify that the $(I_E/I_M)^{\text{TRF}}(f_{\text{free}}=f_{\text{agg}}=0)$ ratio scales as $50 \times \langle k \rangle^{0.95}$ as observed for 64 PyLMs in THF.¹⁵ The ratio $(I_E/I_M)^{\text{TRF}}(f_{\text{free}}=f_{\text{agg}}=0)$ is obtained by setting $f_{E0} = f_D = f_{\text{free}} = 0$ in Equation 3. This condition ensures that the $(I_E/I_M)^{\text{TRF}}(f_{\text{free}}=f_{\text{agg}}=0)$ ratio represents solely those pyrenyl labels that form excimer by diffusion as $\langle k \rangle$ also does. The trend shown in Figure 3B suggests that the parameters retrieved from the MFA of the monomer and excimer TRF decays follow the scaling relationship expected for any PyLMs in THF. At this stage, all the validation criteria had been fulfilled and the parameters retrieved from the MFA of the decays were deemed credible.

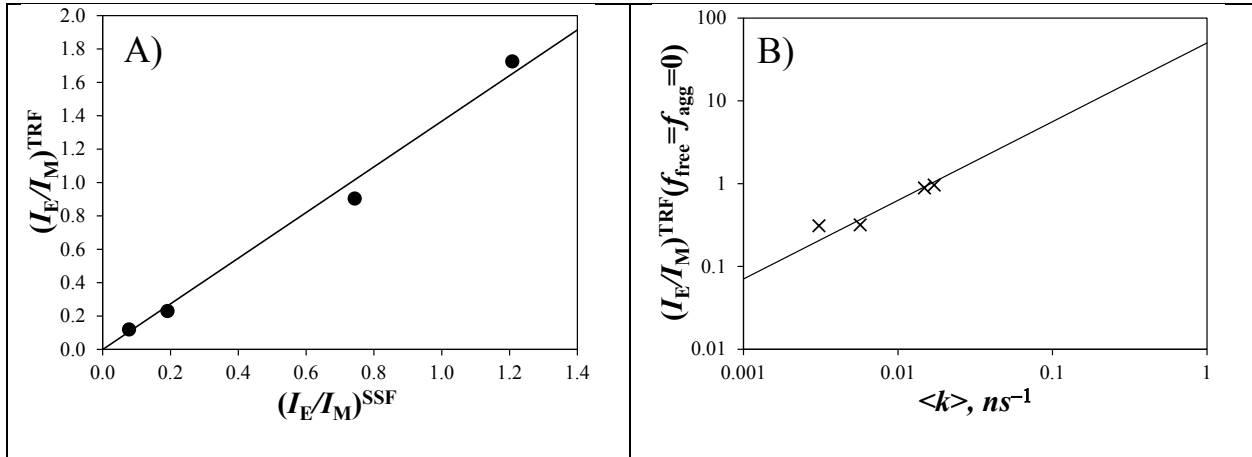


Figure 3. A) Plot of the absolute $(I_E/I_M)^{\text{TRF}}$ ratio obtained by MFA of the TRF decays as a function of the relative $(I_E/I_M)^{\text{SSF}}$ ratio obtained from the analysis of the SSF spectra for the Py-PIMA samples. B) Plot of $(I_E/I_M)^{\text{TRF}}(f_{\text{free}}=f_{\text{agg}}=0)$ as a function of $\langle k \rangle$ for the Py-PIMA samples and how they compare with the master curve $(I_E/I_M)^{\text{TRF}}(f_{\text{free}}=f_{\text{agg}}=0) = 50 \times \langle k \rangle^{0.95}$.

The molar fractions f_{diff} , f_{free} , and f_{agg} obtained from the MFA of the decays were plotted in Figure 4B as a function of the molar percentage of pyrenyl-labeled structural units in Py-PIMA. With a pyrenyl content of 5 mol%, f_{free} and f_{agg} equalled 0.47 and 0.10, respectively. At this low pyrenyl content, many pyrenyl groups were isolated and could not form an excimer. Consequently, the monomer fluorescence intensity I_M used to determine $(I_E/I_M)^{\text{SSF}}$ is dominated by pyrenyl monomers that do not form excimer and, as such, do not reflect pyrenyl excimer formation. As the pyrenyl content increased from 5 to 47.5 mol%, f_{free} and f_{agg} continuously decreased and increased, respectively. At a pyrenyl content of 47.5 mol%, f_{free} and f_{agg} equalled 0.03 and 0.48, respectively. At this high pyrenyl content, close to 50% of the pyrenyl labels were pre-associated and formed excimer quasi instantaneously upon direct excitation in a process that does not reflect the LRPCD of PIMA. In this case, the fluorescence intensity I_E for the excimer that is used to determine $(I_E/I_M)^{\text{SSF}}$ no longer reflects excimer formation by diffusive encounters between two pyrenyl labels. These considerations raise obvious concerns about the interpretation of fluorescence spectra for the characterization of the LRPCD of stiff polymers like PIMA.

The progressive increase in f_{agg} observed in Figure 4, from 0.10 to 0.48 with increasing pyrenyl content, is consistent with the increased difference $\Delta P = P_M - P_E$ in the peak-to-valley ratios between the pyrenyl monomer (P_M) and excimer (P_E) reported earlier.²¹ The peak-to-valley ratios are obtained from the excitation fluorescence spectrum as the ratios between the fluorescence intensities at the peak maxima for the 0-0 vibronic band at 344 nm and the minima separating them from the next higher 0-1 vibronic band of the $S_0 \rightarrow S_2$ transition.

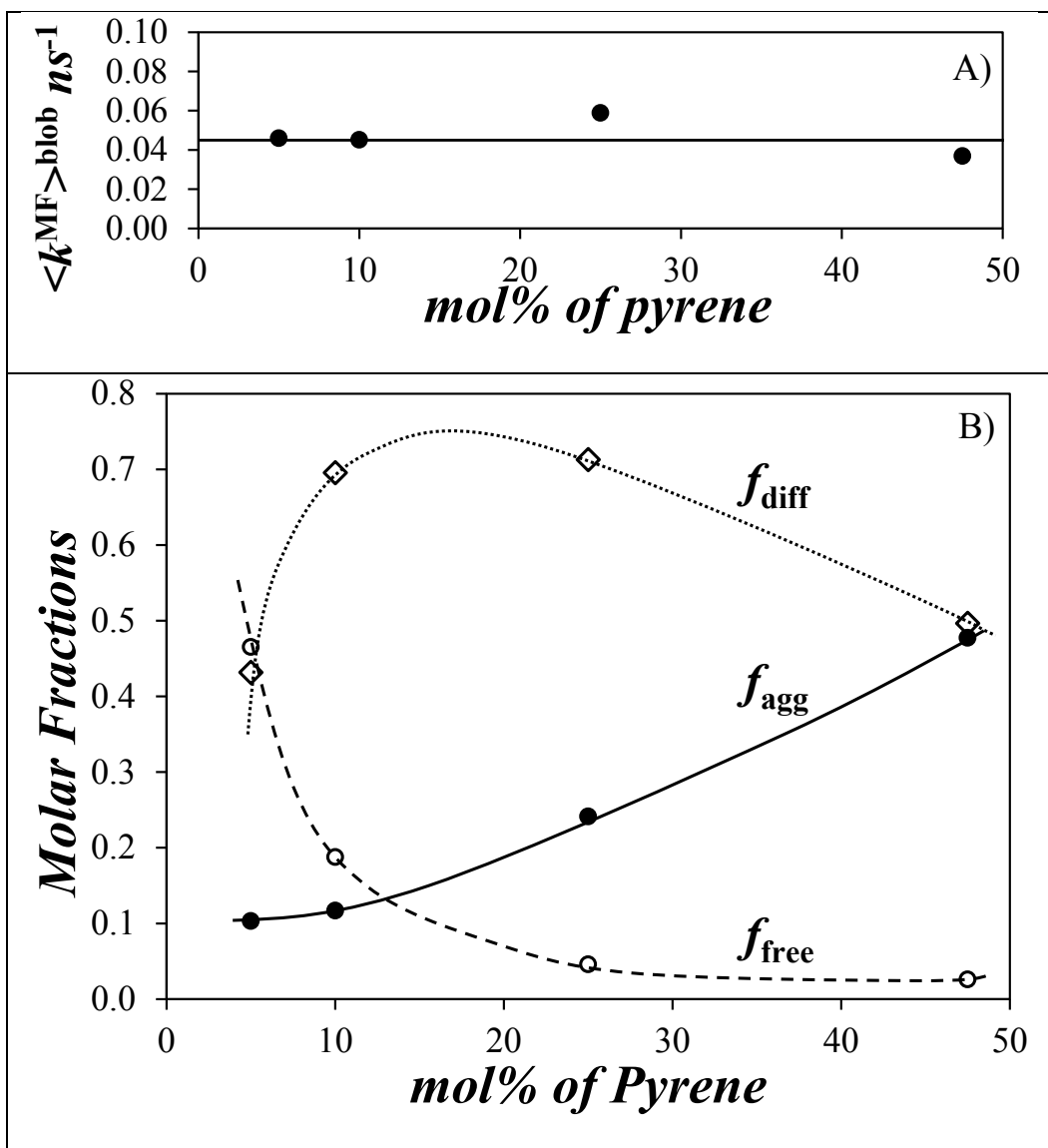


Figure 4. Plot of A) $\langle k \rangle^{\text{MF}}$ and B) f_{free} , f_{diff} , and f_{agg} as a function of the molar percentage of pyrenyl-labeled structural units in Py-PIMA.

The P_M and P_E values are derived from excitation spectra obtained by monitoring the emission intensities corresponding to the monomer (377 nm) and excimer (480 nm), respectively. If there is no ground-state aggregation of pyrenyl groups, so that the excimer is generated through the excitation of the monomer, P_M is equal to P_E , and $\Delta P = \text{zero}$. Direct excitation of pyrenyl aggregates opens a new pathway to excimer formation which results in smaller P_E and positive ΔP

values ΔP for Py-PIMA was found to increase from 0.20 to 0.45 with increasing pyrenyl content.²¹ This trend can be rationalized qualitatively by increasing pyrenyl aggregation, and is confirmed quantitatively by the data in Figure 4.

The f_{free} value of 0.47 determined for Py-PIMA with 5 mol% of pyrenyl substitution was considerably larger than the f_{free} value obtained at a same pyrenyl content for any other polymer randomly labeled with pyrenyl groups studied to date in THF.^{10,11,14-20} One possible reason for this result might be that the PIMA sample is relatively short with a weight-average DP of 78. Short chains might favour the compartmentalization of the pyrenyl labels among different PIMA molecules, resulting in a large f_{free} value. However, if compartmentalization of the pyrenyl groups was a problem, large f_{free} values would be observed at all pyrenyl contents. Since f_{free} approaches zero and equals 0.05 and 0.03 for pyrenyl content of 25 and 47.5 mol%, respectively, the PIMA sample used for the labeling must be constituted of chains that are large enough to host more than one pyrenyl label and as such, represents a good substrate to probe the LRPCD of PIMA. The large f_{free} value observed at low pyrenyl content is most likely due to the stiff PIMA backbone that prevents diffusive encounters between pyrenyl labels as was inferred from the analysis of the SSF spectra in Figure 1A.

Although expected, the trends observed for the molar fractions in Figure 4B also represent a wide variation in the population of the different pyrenyl species which in turn affects the analysis of the SSF spectra. In fact, between 29 and 57% of the pyrenyl labels, depending on the pyrenyl content, did not form excimer by diffusion in the Py-PIMA samples. Together, these observations raise concerns about the accuracy of an analysis based solely on the parameter $m(I_E/I_M)$ obtained from the analysis of SSF spectra. While $m(I_E/I_M)$ is rather small for the PIMA samples reflecting the stiffness of the backbone, the use of $m(I_E/I_M)$ alone to assess the relative stiffness of PIMA

with respect to other polymeric backbones might not be very accurate. This is where the MFA provides a more robust characterization of LRPCD.

In contrast to an analysis based on $m(I_E/I_M)$, the MFA yields the average rate constant $\langle k \rangle$ that solely represents the dynamics experienced by the pyrenyl labels forming excimer by diffusion. Because $\langle k \rangle$ is proportional to the local pyrenyl concentration experienced by an excited pyrenyl group in the polymer coil, $\langle k \rangle$ increases with increasing pyrenyl content, as the I_E/I_M ratio does, which makes it difficult to assess which $\langle k \rangle$ value best represents the LRPCD of the polymer of interest. This problem can be circumvented by using $\langle k \rangle$ to determine $\langle k^{MF} \rangle^{blob}$ according to Equation 6 where x represents the mole fraction of pyrenyl-labeled structural units in Py-PIMA. $\langle k^{MF} \rangle^{blob}$ has been shown to provide a quantitative and reliable representation of LRPCD that is similar to that obtained with the fluorescence blob model (FBM), a well-established procedure.^{6,8,9,23} The FBM compartmentalizes the macromolecular volume into a cluster of *blobs* among which the pyrenyl labels distribute themselves randomly according to a Poisson distribution. A *blob* is defined as the subvolume inside the macromolecular volume probed by a pyrenyl label while it remains excited. Analysis of the TRF decays according to the FBM yields N_{blob} , the average number of structural units found inside a *blob*, and k_{blob} , the rate constant describing the diffusive encounters between two structural units bearing a pyrenyl label.^{8,9} The product $k_{blob} \times N_{blob}$ obtained from the FBM analysis of TRF decays has been found to faithfully describe the LRPCD of numerous polymers¹⁷⁻²⁰ and $\langle k^{MF} \rangle^{blob}$ determined from the MFA yields values similar to $k_{blob} \times N_{blob}$.

$$\langle k^{MF} \rangle^{blob} = \frac{1 - f_{Mfree}}{x} \langle k \rangle \quad (6)$$

$\langle k^{\text{MF}} \rangle^{\text{blob}}$ was calculated and plotted as a function of pyrenyl content in Figure 4A. It remained constant within experimental error and equal to $4.7 (\pm 0.9) \times 10^7 \text{ s}^{-1}$. The constancy of $\langle k^{\text{MF}} \rangle^{\text{blob}}$ over such a wide range of pyrenyl contents is quite remarkable when considering the wide variation in the populations of the different pyrenyl species (see Figure 4B). Interestingly, increasing the pyrenyl content would have been expected to increasingly slow the LRPCD of the labeled PIMA. The lack of such an effect in Figure 4A suggests that the succinic anhydride ring is already so rigid that replacing it with 1-pyrenylmethylsuccinimide does not affect the LRPCD.

In order to rank the LRPCD of PIMA, the values of $\langle k^{\text{MF}} \rangle^{\text{blob}}$ that have been obtained to date with different polymers are summarized in Figure 5, where $\langle k^{\text{MF}} \rangle^{\text{blob}}$ is plotted as a function of the molar mass of the average structural unit (M_0) of the different polymers investigated so far in THF. The chemical structures of these polymers are listed in Table 1. In Figure 5, the hollow symbols refer to polymers that were labeled with a 1-pyrenylbutyl derivative. The PyBut-X(6)-PCyMA series was the most complete and is represented by circles. The $\langle k^{\text{MF}} \rangle^{\text{blob}}$ value obtained with the poly(alkyl methacrylate)s follows the expected trend, whereby a bulkier side chain results in slower LRPCD and a reduced $\langle k^{\text{MF}} \rangle^{\text{blob}}$ value. Polystyrene (PyBut-X(6)-PS), represented by squares, shares the same $\langle k^{\text{MF}} \rangle^{\text{blob}}$ value as PyBut-X(6)-PC1MA as would be expected since these two polymers have a similar T_g values and, thus, similar main-chain dynamics. Another reason for considering polystyrene is that it represents an important reference point for the experimental determination of LRPCD. Polystyrene has been argued to be the stiffest backbone that could be probed by conducting EEC fluorescence quenching experiments.⁶ As can be seen in Figure 5, all polymers considered in this study have $\langle k^{\text{MF}} \rangle^{\text{blob}}$ values that are smaller than for polystyrene so that their LRPCD could not be characterized by the standard EEC fluorescence quenching procedure.

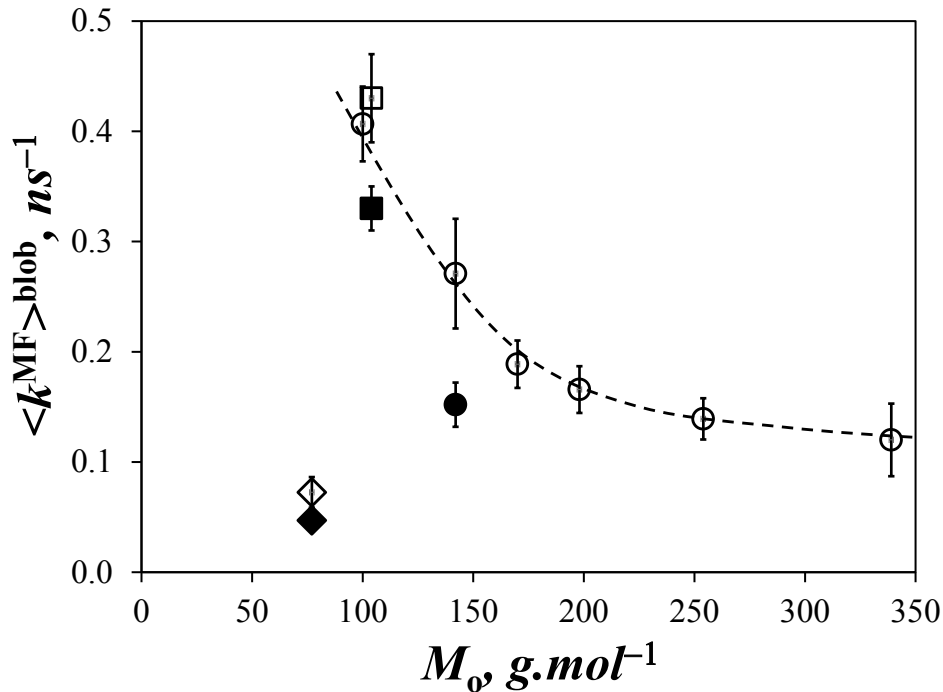


Figure 5. Plot of $\langle k^{\text{MF}} \rangle^{\text{blob}}$ as a function of the molar mass of the structural unit (M_0). (○) PyBut-X(6)-PCyMA series with $y = 1, 4, 6, 8, 12,$ and $18,$ (●) PyMeO-X(3)-PC4MA, (□) PyBut-X(6)-PS, (■) PyMeN-X(3)-PS, (◆) Py-PIMA, (◇) Py-PIMA scaled by 1.54.

It is obvious from the location of the diamond symbols in Figure 5 representing $\langle k^{\text{MF}} \rangle^{\text{blob}}$ for Py-PIMA that the PIMA backbone experiences very slow LRPCD. However, this statement needs to be qualified by noting that, whereas the $\langle k^{\text{MF}} \rangle^{\text{blob}}$ values reported with hollow symbols were obtained for polymers labeled with a 1-pyrenylbutyl derivative, the pyrenyl labels are much closer to the main chain for Py-PIMA. The effect of shortening the linker connecting pyrenyl to the chain is known to decrease $\langle k^{\text{MF}} \rangle^{\text{blob}}$ as illustrated in Figure 5 for PyMeN-X(3)-PS¹⁴ and for PyMeO-X(3)-PC4MA¹¹ whose $\langle k^{\text{MF}} \rangle^{\text{blob}}$ (filled square and circle in Figure 5) decreased by 30 and 78%, respectively, upon replacing a 6-atom linker by a 3-atom linker. This effect could be partially

accounted for by scaling the $\langle k^{MF} \rangle^{blob}$ value of Py-PIMA by 1.54 (equivalent to the average of 1.3 and 1.78) as shown in Figure 5 (unfilled diamonds).

Despite this adjustment, the scaled $\langle k^{MF} \rangle^{blob}$ value of Py-PIMA remained much smaller than all others reported in Figure 5. In fact, polymers with such a low M_0 value would be expected to exhibit fast LRPCD that should yield a $\langle k^{MF} \rangle^{blob}$ value in the upper left corner of Figure 5 contrary to what was observed for Py-PIMA. Consequently this study leads to the conclusion that the succinic anhydride rings in the PIMA backbone slow its LRPCD considerably. The slow LRPCD of PIMA would reduce the number of EEC events to an undetectable level that would prevent the application of EEC fluorescence quenching experiments for their characterization. Furthermore, the preparation of PIMA by free radical copolymerization of isobutylene and maleic anhydride does not lend itself to the incorporation of reactive groups at the chain ends, a strict requirement to characterize the LRPCD of a polymer by studying the EEC of its chains by fluorescence quenching, the classic procedure to date. Such considerations highlight the importance of experimental procedures such as the fluorescence blob model (FBM) or MFA which enables the study of LRPCD of stiff polymers^{8,9} that could not be otherwise investigated experimentally by classic EEC fluorescence quenching experiments.^{5,6}

CONCLUSIONS

This study has successfully demonstrated that the LRPCD of PIMA can be described quantitatively through the careful analysis of the TRF decays of five PIMA samples randomly labeled with pyrenyl groups. The monomer and excimer TRF decays were fitted globally according to the MFA which yielded the molar fractions of the different pyrenyl species found in solution (i.e., f_{free} , f_{diff} , and f_{agg}). as well as the average rate constant $\langle k \rangle$ of pyrenyl excimer formation, and the absolute

fluorescence intensity ratio $(I_E/I_M)^{\text{TRF}}$. One superior feature of the MFA is that the validity of the parameters recovered through fitting the fluorescence decays can be confirmed by checking first, that the absolute $(I_E/I_M)^{\text{TRF}}$ ratios obtained from Equation 3 are proportional to the $(I_E/I_M)^{\text{SSF}}$ ratios obtained from the analysis of the SSF spectra and, second, that $(I_E/I_M)^{\text{TRF}}(f_{\text{free}}=f_{\text{agg}}=0)$ scales as $50 \times \langle k \rangle^{0.95}$ as has been already reported for 64 other PyLMs in THF.¹⁵ To the best of our knowledge, the MFA seems to be the only analysis method of fluorescence decays reported in the literature that provides such stringent checks to assess the validity of the kinetic parameters it retrieves.

Having successfully passed these checks (N. B., Figure 3), the MFA parameters could then be investigated in earnest. The molar fractions f_{free} and f_{agg} were found to decrease continuously and increase, respectively, with increasing pyrenyl content. While these trends were expected, they also led to the conclusions that between 30 and 70% of the pyrenyl labels formed excimer by diffusion, so that the sole analysis of the SSF spectra to gain information about the LRPCD of PIMA would certainly lead to erroneous results. By contrast, MFA of the TRF decays enabled us to isolate the contribution of the pyrenyl labels forming excimer by diffusion and that would most closely reflect the LRPCD of PIMA. This analysis yielded the parameter $\langle k^{\text{MF}} \rangle^{\text{blob}}$, which has been shown to report faithfully the LRPCD.^{14,15} Comparison of $\langle k^{\text{MF}} \rangle^{\text{blob}}$ for PIMA with the $\langle k^{\text{MF}} \rangle^{\text{blob}}$ value of 9 other polymers in THF indicates that PIMA exhibits extremely slow LRPCD, particularly for a polymer constituted of a low molecular weight structural unit (see Figure 5). Although such a conclusion is not very surprising based on the chemical structure of PIMA, the importance of this result revolves more around the protocol outlined in this report which demonstrates that information about the LRPCD of stiff polymeric backbones can be retrieved quantitatively in a form that enables one to rank different polymeric backbones according to their

relative stiffness. That such information is obtainable with a polymer as stiff as PIMA, whose LRPCD would be challenging to determine by EEC fluorescence quenching study, suggests that it can also be applied to characterize the LRPCD of even more complex backbones such as those of polypeptides whose LRPCD are highly relevant for the study of protein folding.

ACKNOWLEDGEMENTS

JLT and JD thank NSERC for generous funding. MJL, MJB, and RGW thank the US National Science Foundation for its support of this research through Grant CHE-1502856. MJL also acknowledges a scholarship administered by the Education Department of Fujian Province, P. R. China and the support by the National Scientific Foundation of China (NSFC No. 21171038).

SUPPORTING INFORMATION

Derivation of the molar fractions of the different pyrenyl species; parameters retrieved from the MFA of the monomer and excimer TRF decays.

REFERENCES

1. Brucale, M.; Schuler, B.; Samori, B. Single-Molecule Studies of Intrinsically Disordered Proteins. *Chem. Rev.* **2014**, *114*, 3281-3317.
2. Sustarsic, M.; Kapanidis, A. N. Taking the Ruler to the Jungle: Single-Molecule FRET for Understanding Biomolecular Structure and Dynamics in Living Cells. *Curr. Opin. Struct. Biol.* **2015**, *34*, 52-59.
3. Haas, E. The Study of Protein Folding and Dynamics by Determination of Intramolecular Distance Distributions and Their Fluctuations Using Ensemble and Single-Molecule FRET Measurements. *ChemPhysChem* **2005**, *6*, 858-870.

4. Schuler, B.; Soranno, A.; Hofmann, H.; Nettels, D. Single-Molecule FRET Spectroscopy and the Polymer Physics of Unfolded and Intrinsically Disordered Proteins. *Ann. Rev. Biophys.* **2016**, *45*, 207-231.
5. Winnik, M. A. End-to-End Cyclization of Polymer Chains. *Acc. Chem. Res.* **1985**, *18*, 73-79.
6. Farhangi, S.; Duhamel, J. Long Range Polymer Chain Dynamics Studied by Fluorescence Quenching. *Macromolecules* **2016**, *49*, 6149-6162.
7. Svirskaya, P.; Danhelka, J.; Redpath, A. E. C.; Winnik, M. A. Cyclization Dynamics of Polymers: 7. Applications of the Pyrene Excimer Technique to the Internal Dynamics of Polydimethylsiloxane Chains. *Polymer* **1983**, *24*, 319-322.
8. Duhamel, J. Global Analysis of Fluorescence Decays to Probe the Internal Dynamics of Fluorescently Labeled Macromolecules. *Langmuir* **2014**, *30*, 2307-2324.
9. Duhamel, J. New Insights in the Study of Pyrene Excimer Fluorescence to Characterize Macromolecules and their Supramolecular Assemblies in Solution. *Langmuir* **2012**, *28*, 6527-6538.
10. Farhangi, S.; Duhamel, J. A Pyrenyl Derivative with a Four Atom-Linker that Can Probe the Local Polarity of Pyrene-Labeled Macromolecules. *J. Phys. Chem. B* **2016**, *120*, 834-842.
11. Farhangi, S.; Duhamel, J. Probing Side Chain Dynamics of Branched Macromolecules by Pyrene Excimer Fluorescence. *Macromolecules* **2016**, *49*, 353-361.
12. Siu, H.; Duhamel, J. Comparison of the Association Level of a Hydrophobically Modified Associative Polymer Obtained from an Analysis Based on Two Different Models. *J. Phys. Chem. B* **2005**, *109*, 1770-1780.

13. Yip, J.; Duhamel, J.; Bahun, G.; Adronov, A. A Study of the Branch Ends of a Series of Pyrene-Labeled Dendrimers Based on Pyrene Excimer Formation. *J. Phys. Chem. B* **2010**, *114*, 10254-10265.
14. Fowler, M. A.; Duhamel, J.; Bahun, G. J.; Adronov, A.; Zaragoza-Galán, G.; Rivera, E. Studying Pyrene-Labeled Macromolecules with the Model Free Analysis. *J. Phys. Chem. B* **2012**, *116*, 14689-14699.
15. Farhangi, S.; Casier, R.; Li, L.; Thoma, J.; Duhamel, J. Characterization of the Long Range Internal Dynamics of Pyrene-Labeled Macromolecules by Pyrene Excimer Fluorescence. *Macromolecules* **2016**, *49*, 9597-9604.
16. Ingratta, M.; Hollinger, J.; Duhamel, J. A Case for Using Randomly Labeled Polymers to Study Long Range Polymer Chain Dynamics by Fluorescence. *J. Am. Chem. Soc.* **2008**, *130*, 9420-9428.
17. Ingratta, M.; Mathew, M.; Duhamel, J. How Switching the Substituent of a Pyrene Derivative from a Methyl to a Butyl Affects the Fluorescence Response of Polystyrene Randomly Labeled with Pyrene. *Can. J. Chem.* **2010**, *88*, 217-227.
18. Farhangi, S.; Weiss, H.; Duhamel, J. Effect of Side-Chain Length on the Polymer Chain Dynamics of Poly(alkyl methacrylate)s in Solution. *Macromolecules* **2013**, *46*, 9738-9747.
19. Kanagalingam, S.; Spartalis, J.; Cao, T.-C.; Duhamel, J. Scaling Relations Related to the Kinetics of Excimer Formation between Pyrene Groups Attached onto Poly(N,N-dimethylacrylamide)s. *Macromolecules* **2002**, *35*, 8571-8577.
20. Yip, J.; Duhamel, J.; Qiu, X. P.; Winnik, F. M. Long-Range Polymer Chain Dynamics of Pyrene-Labelled Poly(N-isopropylacrylamide)s Studied by Fluorescence. *Macromolecules* **2011**, *44*, 5363-5372.

21. Li, M.-J.; Bertocchi, M. J.; Weiss, R. Photophysics of Pyrenyl-Functionalized Poly(isobutylene-*alt*-maleic anhydride) and Poly(isobutylene-*alt*-maleic N-alkylimide). Influence of Solvent, Degree of Substitution, and Temperature. *Macromolecules* in press (DOI: 10.1021/acs.macromol.6b02434).
22. Chen, S.; Duhamel, J.; Bahun, G.; Adronov, A. Effect of Fluorescent Impurities in the Study of Pyrene-Labeled Macromolecules by Fluorescence. *J. Phys. Chem. B* **2011**, *115*, 9921-9929.
23. Duhamel, J. Polymer Chain Dynamics in Solution Probed with a Fluorescence Blob Model. *Acc. Chem. Res.* **2006**, *39*, 953-960.

Table of Content

**Rigid-vs-Flexible Backbones Probed by
Pyrene Excimer Fluorescence**

